NanoTBTech

Nanoparticles-based 2D thermal bioimaging technologies

H2020-FETOPEN-1-2016-2017

Grant Agreement: 801305

Deliverable number D1.2 (D2)

Powder-to-colloidal nanoparticles protocol

Final Version

Project Deliverable Information Sheet

NanoTBTech Project	Project Ref. No. 801305
	Project Title: *Nanoparticles-based 2D thermal bioimaging technologies*
	Project Website: http://www.nanotbtech.eu/
	Deliverable No.: D2
	Deliverable Type: Report
	Dissemination Level: Public
	Contractual Delivery Date: 31 May 2019
	Actual Delivery Date: 31 May 2019
	EC Project Officer: Barbara GERRATANA

Document Control Sheet

Document	Title: Powder-to-colloidal nanoparticles protocol
	Version: Final
	Available at: Participant's Portal
Authorship	Written by: INSTYTUT NISKICH TEMPERATUR I BADAN STRUKTURALNYCH IM. WLODZIMIERZA TRZEBIATOWSKIEGO POLSKIEJ AKADEMII NAUK (WPAS)
	Contributed by: - INSTITUT ZA NUKLEARNE NAUKE VINCA (VINCA) - UNIVERSIDADE DE AVEIRO (UAVR) - CENTRE NATIONAL DE LA RECHERCHE SCIENTIFIQUE CNRS (CNRS) - AGENCIA ESTATAL CONSEJO SUPERIOR DEINVESTIGACIONES CIENTIFICAS (CSIC) - UNIVERSITEIT UTRECHT (UU)
	Approved by: all partners

History of Changes

Version	Date	Description	Reviewer
V0	17.04.2019.	Version 0	WPAS
V1	14.05.2019	Version 1	WPAS, VINCA, CNRS
V2	27.05.2019	Version 2	Prof. Luis Carlos
Final Version	27.05.2019	Final Version	All partners

*This project has received funding from the European Union's Horizon 2020 research and innovation programme under grant agreement No **801305.***

Abbreviations and Acronyms

ABCP	Amphiphilic block copolymer
AIBN	Azobisisobutyronitrile
AuNPs	Gold nanospheres
AuNRs	Gold nanorods
BTFA	Bis Trifluoroacetamide
BW	Biological window
CA	Citric acid
CNRS	Centre National de la Recherche Scientifique
COD	Crystallography Open Database
CSIC	Agencia Estatal Consejo Superior de Investigaciones Cientificas
CTA	Chain Transfer Agent
CTAB	Cetyl trimethylammonium bromide
DLS	Dynamic light scattering
DNPD	1,3-di(naphthalen-2-yl)propane-1,3-dione
EG	Ethylene glycol
FIBIRYCIS	Fundacion para la Investigacion Biomedica del Hospital Universitario Ramon Y Cajal
FWHMs	Full widths at half maximum
GOF	Goodness of fit
^{1}H-NMR	Proton nuclear magnetic resonance
HR-TEM	High-resolution transmission electron microscopy
ICDD	International Centre for Diffraction Data
ICP- AES	Inductively Coupled Plasma - Atomic Emission Spectrometry
ICSD	Inorganic Crystal Structure Database
Ln^{3+}	Lanthanide ions
LPO	$LaPO_4$
MA	Methyl acrylate
MPA	3-mercaptopropionic acid
MPEGA	Metoxy-Polyethylene glycol acid

*This project has received funding from the European Union's Horizon 2020 research and innovation programme under grant agreement No **801305.***

MWCO	Molecular weight cut-off
NIR	Near Infra-Red
NPO	$NdPO_4$
NPs	Nanoparticles
NTMs	Nanothermometer
NHs	Nanoheater
OA	Oleic acid
ODE	Octadecene
PEGA	Polyethylene glycol acid
PhenA	(1,10-phenanthrolin-4-yl)methyl acrylate
PL	Photoluminescence
PTFE	Polytetrafluoroethylene
QDs	Quantum dots
RAFT	Reversible addition-fragmentation chain transfer polymerization
Re	Expected weighted profile factor (Re)
Rp	Profile factor
Rwp	Weighted profile factor
SPR	Surface Plasmon Resonance
TEM	Transmission electron microscopy
TEOS	Tetraethoxysilan
THF	Tetrahydrofuran
TM	Transition metal
UAVR	Universidade de Aveiro
UCNPs	Upconverting nanoparticles
UU	Universiteit Utrecht
UV-VIS	Ultraviolet–visible spectroscopy
VINCA	Institut Za Nuklearne Nauke Vinca
WP	Work package(s)
WPAS	Instytut Niskich Temperatur I Badan Strukturalnych Im. Wlodzimierza Trzebiatowskiego Polskiej Akademii Nauk
XRD	X-Ray Diffraction

*This project has received funding from the European Union's Horizon 2020 research and innovation programme under grant agreement No **801305.***

YAG Yttrium aluminium garnet ($Y_3Al_5O_{12}$)

YIG Yttrium iron garnet ($Y_3Fe_5O_{12}$)

*This project has received funding from the European Union's Horizon 2020 research and innovation programme under grant agreement No **801305.***

*This project has received funding from the European Union's Horizon 2020 research and innovation programme under grant agreement No **801305.***

Table of Contents

*This project has received funding from the European Union's Horizon 2020 research and innovation programme under grant agreement No **801305.***

D1.2 Protocol describing the synthesis methodology for developing colloidal NPs suitable for bio-applications in the NIR spectral region

The goal of the NanoTBTech project is to develop a 2-D thermal bioimaging technology featuring sub-microscale resolution, based on nanothermometers and heater-thermometer nanostructures. We will design, synthetize, and bio-functionalize nontoxic luminescent nanostructures, operating essentially beyond 1000 nm, for in vivo nanothermometry and nanoheating. Furthermore, to monitor the temperature-dependent nanostructures' luminescence we will develop a novel imaging system. The effective delivery of that major advance in 2-D thermal bioimaging will be implemented through two impactful biomedical showcases: highly spatially-modulated intracellular magnetic/optical hyperthermia and in vivo detection and tracking of cancer. Multiple conceptual breakthroughs can be further envisaged from the proposed 2D-thermal imaging system, credibly spreading its impact towards nonbiomedical technological areas.

Work package 1 (WP1) of the project is titled: "Design and synthesis of luminescent NPs and heater-thermometer nanostructures". The report is mainly given by INSTYTUT NISKICH TEMPERATUR I BADAN STRUKTURALNYCH IM. WLODZIMIERZA TRZEBIATOWSKIEGO POLSKIEJ AKADEMII NAUK (WPAS), with a strong support of all other partners of the WP1 leaded by INSTITUT ZA NUKLEARNE NAUKE VINCA (VINCA):

- UNIVERSIDADE DE AVEIRO (UAVR)
- CENTRE NATIONAL DE LA RECHERCHE SCIENTIFIQUE CNRS (CNRS)
- AGENCIA ESTATAL CONSEJO SUPERIOR DEINVESTIGACIONES CIENTIFICAS (CSIC)
- UNIVERSITEIT UTRECHT (UU)

This report describes the reasons and protocols, as well as the first results on colloidal nanoparticles, which are co-doped with lanthanide (Ln^{3+}) and transition metal (TM). Report consists of synthesis and basic characterization of purposeful materials examined so far aiming to provide specifically information on colloidal materials, as only these materials are suitable for further biomedical applications.

*This project has received funding from the European Union's Horizon 2020 research and innovation programme under grant agreement No **801305.***

1. General reasons to produce colloidal nanoparticles

Temperature is one of the most frequently measured physical quantity. Beaside technology, microelectronics, mechanics and engineering, temperature measurements are also very important in biomedical sciences. Our aim motivation is to develop technology, suitable to perform feedback controlled hyperthermia treatment of cells and whole tissues/organs. This means, not only 2-D thermal bioimaging technology featuring sub-microscale resolution has to be developed, but also non-invasive observation through the tissue condition must be satisfied. Despite numerous reliable technologies exists which enable to measure or map temperature, they are not suitable for our purposes. For example thermocouple allows for single spot measurements only and does not allow for intratumoral temperature monitoring without invasive injection of the probe into the tissue. Bolometric termovision camera, exploits IR emission of the samples (7-14 mm), which is then converted to temperature maps. The major drawbacks of this technology are the facts it can only visualise the temperature of the surface of the object (e.g. skin) and the principle of operation of the TV cameras does not fit conventional optical instrumentation (e.g. optical microscopes). We plan to solve these issues by employing luminescent biofunctionalied nanoparticles to serve as luminescent temperature sensors (i.e. nano-thermometers NTMs) and light-to-heat converters (i.e.nano-heaters NHs). The fundamental requirement for these materials is to get them in nanocolloidal form. This is because NTMs and NHs must be biofunctionalized prior the application to target specific organs and tissues (in vivo) or molecules (in vitro) to report the temperature from treated sites. The nanocolloidal particles must have freedom to circulate in the body (in vivo) and to potentially penetrate membranes of living cells (in vitro), and only the nanoparticles, whose diameter does not exceed 50 nm can satisfy these requirements.

One may summarize the main goals for the scientific community to bring nanotechnology to bedside, and specifically for us to demonstrate temperature mapping in-vitro and in-vivo:

- Stabilize the nanoparticles (NPs) in aqueous and biological media
- Reduce the recognition by the mononuclear phagocyte system (MPS)
- Design an active targeting to improve tumor uptake

The NPs of interest, either nano-heaters (NH) or nano-thermometer (NT) are made of numerous different matrixes such as:

- Fluor: AF_2, (A=Ca, Sr, Ba), $Na(Y, Gd, Lu)F_4$, $NaNdF_4$
- Oxides: Y_2O_3, Fe_2O_3, Fe_3O_4, $Y_3Fe_5O_{12}$
- Phosphate: $LiLaP_4O_{12}$
- Quantum dots : Ag_2S, Ag_2Se

*This project has received funding from the European Union's Horizon 2020 research and innovation programme under grant agreement No **801305.***

2. Short state-of-the-art in making colloidal NPs

Several reports have described efficient synthesis approaches to produce the shape-controlled, stable, colloidal and monodispersed NPs.

Metal NPs are typically prepared in solution by reduction of metal salts with chemical reducing agents or photoreduction. The size and shape of the metal NPs are typically controlled through the judicious choice of concentration, reducing agent, and ligand.

Semiconductor NPs are synthesized using a variety of different synthetic approaches. QDs are typically synthesized at high temperatures by combining the metal and chalcogenide precursors as salts and heating to high temperatures (>300 °C) in the presence of a capping agent (often long chain carboxylic acids or trioctyl phosphine oxide) under inert atmosphere conditions. In addition to controlling the size and shape of the QDs, it is also essential to preserve the quality of their surface, as vacancies and faults in the surface can negatively impact their fluorescence and excitation properties. Metal oxide NPs, in contrast, are typically prepared using base hydrolysis reactions of molecular precursors (frequently acetates) in which the size of the NP is controlled by controlling the rate of hydrolysis versus passivation by the ligand, which is typically a carboxylic acid or functionalized silane. The ligand shell may serve a very different role in the design of semiconductor or insulator NPs. While the ligand shell can still be used as a means to control solubility or target biomacromolecules, the ligand shell can also mediate the electronic properties of semiconductor NPs (e.g., the longer the chain length of the ligand, the more electronically insulated semiconductor NPs are from their environment).[1]

The one of the most successful and popular methods for the synthesis good quality up-converting NPs are hydro(solvo)thermal and thermal decomposition synthesis. Both methods allow obtaining good quality NPs with precise and narrow size control. Hydrothermal/solvo-thermal method, refers to synthesis procedure within a sealed environment under high pressure and temperature above the critical point of solvent to increase the solubility of solid. The reaction is carried out in reaction vessel (autoclave) to provide sealed reaction condition. The advantage of adopting this method for synthesis of NPs include the ability to create highly crystalline phase at lower temperature and easy control of size, structure and morphology of the NPs. Thermal decomposition reaction has been develop first time by Yan's group to synthesize monodisperse triangular LaF_3 nanoplates,[2] and next refined and extended as a common route to the synthesis of $NaYF_4$ nanocrystals.[3] This method usually involves dissolving organic metal salts (commonly used trifluoroacetate or acetate compounds) in high-boiling point solvents, typically with polar capping groups and long hydrocarbon chains, such as 1-octadecene (ODE, non-coordinating solvent with high boiling point – 315^{o}C), oleic acid (OA), and oleylamine (OM), which perform function of both solvents for the reaction mixture and coordinating agents which stabilize the NPs surface and prevent agglomeration of the particles during the synthesis process. Although the thermal decomposition is demonstrated to be the most effective in controlling the shape and size of NPs, there remains some disadvantages. Resulting NPs are generally only dissolved in nonpolar solvent (e.g. chloroform, hexane), and due to the hydrophobic ligands

*This project has received funding from the European Union's Horizon 2020 research and innovation programme under grant agreement No **801305.***

stabilizing NPs surfaces, post-synthetic functionalization is necessary to transfer the as-synthesized NPs to aqueous solutions and to finally achieve biocompatibility.

General strategies to transform hydrophobic nanoparticles into hydrophilic require inducing or exploiting an existing NPs surface charge. This is achieved either by affixing surface-bound functional groups or the design of appropriate biocompatible coatings. The strategies of surface functionalization of UCNPs can be divided into the following groups: ligand exchange, ligand attraction, ligand oxidation, layer-by-layer assembly, encapsulation in silica shell and host–guest self-assembly (Figure 1).

Ligand exchange

The hydrophobic ligands bound to the UCNP surface can be exchanged by more hydrophilic ligands to form stable aqueous dispersions and introduce functional groups for a subsequent functionalization with biomolecules. In ligand exchange approach, the original hydrophobic ligands are replaced by biofunctional molecules such as polyethylene glycol, polyacrylic acid, hexanedioic acid, thioglycolic acid, citrate. The ligand-exchange preparation reported in the literature is usually a one-step procedure accomplished by directly substituting new ligands for the native ones. The method is simple and the process does not change the shape or a size of NPs, if only the exchange agents are small. The modified UCNPs usually do not show any significant changes in morphology or luminescence emission yield, they do not aggregate and are stable in aqueous solution for long time which makes them ideal candidates for various biological applications. Alternatively the hydrophobic ligands can be removed from the nanoparticles surface without introducing new ligands. This technique is based on pH changes and yields water dispersible UCNPs due to the positively charged nanoparticle surface.[4,5]

Ligand attraction

Ligand attraction involves adsorption of an additional amphiphilic polymer onto the nanocrystal surface through the hydrophobic attraction between the original ligand and hydrocarbon chain of the polymer. The amphiphilic ligand intercalates with the hydrophobic segment of original protecting ligand. The hydrophilic part of the polymer sticks out into the water and permits aqueous dispersion and further bioconjugation. This ligand interaction in an aqueous environment is driven by van-der-Waals interactions between the hydrophobic alkyl chains of the surface ligands and of the amphiphilic compounds such as modified polymers or detergents

Ligand oxidation

Ligand oxidation involves oxidation of double bond between C_9 and C_{10} of the oleic acid by Lemieux-von Rudloff reagent or potassium permanganate to yield azelaic acid and nonanoic acid. The surface attached azelaic acid renders the UCNP surface hydrophilic and enables further conjugation steps.

*This project has received funding from the European Union's Horizon 2020 research and innovation programme under grant agreement No **801305.***

The oxidation has no influence on the size, shape, or crystal phase of the UCNPs. Azelaic acid-coated UCNPs form stable dispersions in water for one week but also in some other polar solvents such as DMSO or DMF. The disadvantage of this strategy is long reaction time and low yield. Moreover, decrease the luminescence intensity of the UCNPs was observed because the relatively short azelaic acid is only insufficiently able to shield the surface from the quenching effects of water.[6]

Layer-by-layer assembly

This method consists of sequential adsorption of oppositely charged polyelectrolytes on NPs surface. LbL assembly seems to be very attractive, being both versatile and simple approach enabling to control the coating thickness of the polyions by choosing the number of layers. Sequential deposition of anionic polyacrylic acid and cationic polyallylaminehydrochloride proved to have good mechanical stability and efficient NIR-to-visible up-conversion luminescence.[7] Bilayer formations were able to shield the upconversion luminescence and thus prevent the disintegration of the nanoparticles even in the phosphate buffer that has been proven to enhance the disintegration.[8]

Encapsulation in silica shell

One of the most frequently used method of UCNPs surface modification is surface silanization. The growth of an amorphous silica shell on the UCNPs involves hydrolysis and condensation of siloxane monomers (e.g. tetraethoxysilane TEOS, 3-aminopropyltriethoxysilane APTES). Silanes provide functional amino or epoxy groups responsible for interfacial properties such as wetting or adhesion. Silica itself is regarded as biocompatible, its surface has been extensively studied and their porosity can be easily controlled. The large surface area and pore volume of mesoporous silica ensure facile adsorption as well as high loading of various therapeutic materials. Typically, there are two routes to coat SiO2 onto UCNPs: one is sol−gel nanochemistry in a reverse micelle nanoreactor to coat SiO2 onto UCNPs with hydrophobic capping ligands. The second is the Stöber method to make SiO2 coating provided that the UCNPs' surfaces have already been modified to be hydrophilic. Unfortunately, some of the reagents used in the course of silica coating are toxic and have to be carefully removed before using the NPs with silica layer in bioassays. Moreover, additional silica layer on the surface of NPs changes the shape and increases the hydrodynamic size of nanoparticles which can be inappropriate for some of biological applications. The precise control over the thickness and shape of the encapsulating SiO2 layer is still an unsolved issue. Another drawback is that the luminescence quantum yield of UCNPs modified with APTES tends to decrease because of free NH2 groups responsible for quenching the emission yield.

Host–guest self-assembly

*This project has received funding from the European Union's Horizon 2020 research and innovation programme under grant agreement No **801305.***

As a typical model of host–guest partners, α-cyclodextrin and oleic acid possess a specific and strong interaction, which has been widely applied to control the surface chemistry of NPs. Usually, oleic acid is first decorated on the NPs, making the NPs dispersible in organic solvents. After mixing with water that contains α-cyclodextrin, α-cyclodextrin can selectively bind with oleic acid to decorate a layer on the NPs, and thus draw the originally hydrophobic NPs into the water.[9] Self-assembly of host molecule and guest molecule has several advantages over other methods because it not only enables to obtain hydrophilic UCNPs but provides a hydrophobic layer for loading a hydrophobic molecules (dyes or drug) as well.

Many functional groups are amenable to improving the dispersibility of UCNPs in water or aqueous buffers such as hydroxyl groups, primary or secondary amines, maleimides, epoxides, carboxylic acids, or phosphonates. Each functionality improves the hydrophilicity to a different extent and especially ionic groups exert a particularly strong influence on the dispersibility. Moreover, the nanoparticle dispersions must be long-term stable in aqueous media to avoid aggregation and precipitation during storage or applications.[10] Dayong Jin's group investigated the competitive adsorption of phosphate, carboxylic acid and sulphonic acid onto the surface of UCNPs and studied their binding strength to identify the best conjugation strategy.[11] Their results showed that the structural and chemical characteristics of ligand groups strongly impact the ligand exchange efficiency with OA capped UCNPs, which in turn influence the colloidal stability of the polymer capped UCNPs in aqueous media. Their experimental finding showed that phosphate ligands lead to the excellent stability of UCNPs for an extended period of time due the complete replacement of OA molecules on the surface and greater absorption energy for phosphate groups with lanthanide ions.[11]

*This project has received funding from the European Union's Horizon 2020 research and innovation programme under grant agreement No **801305.***

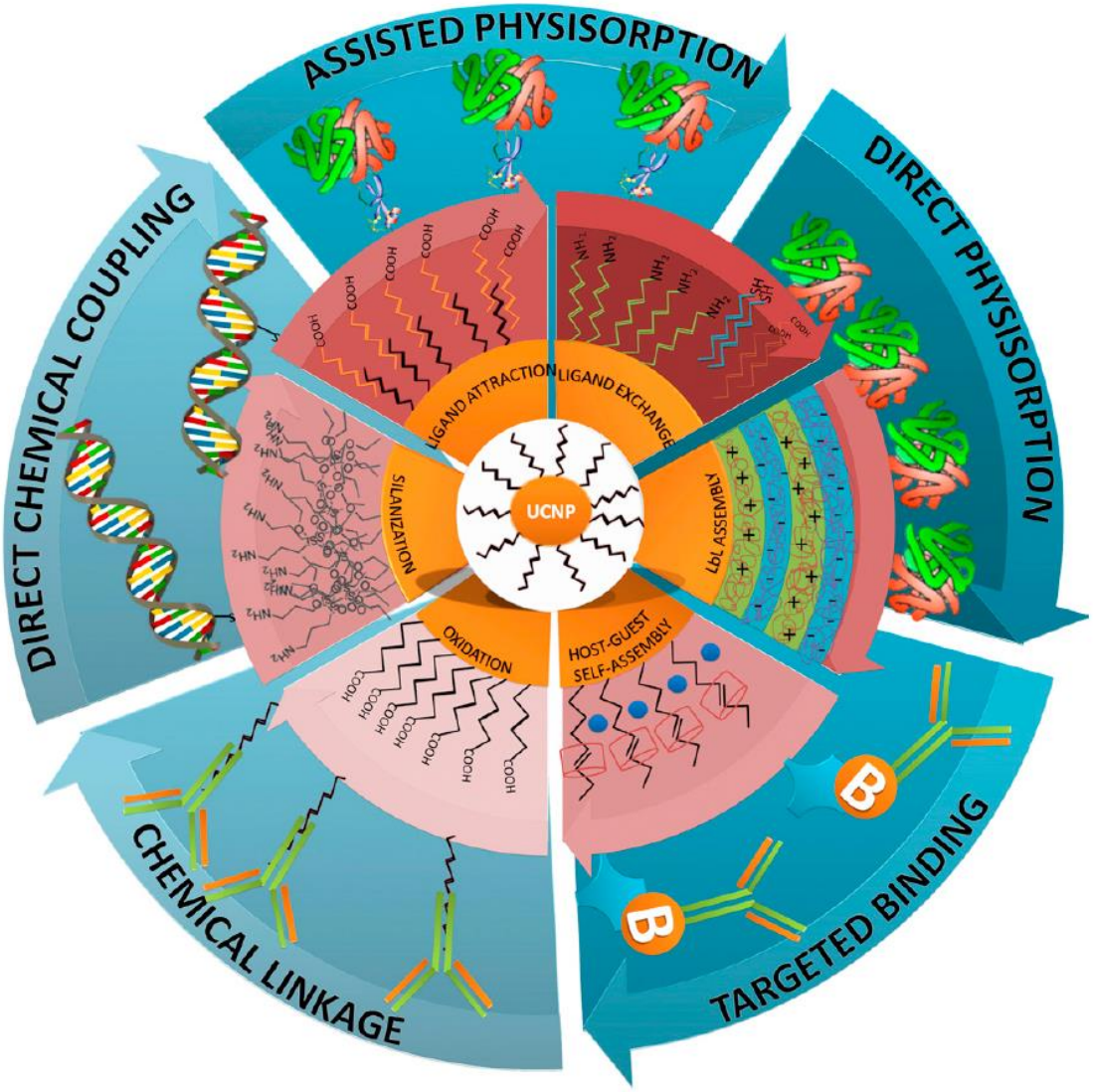

Fig. 1. Schematic representation of strategies of UCNPs surface modification. The first layer relates to surface biofunctionalization: Ligand oxidation, Ligand exchange, Ligand attraction, Silanization, Layer-by-Layer and Host—guest self-assembly. The next step in UCNPs surface modification is bioconjugation with various biomolecules through direct physisorption, assisted physisorption using prebound molecules, chemical linkage of biomolecules to crosslinkers, direct chemical coupling and targeted binding of biotinylated biomolecules to streptavidin coated NPs via biotin—streptavidin coupling (Ref.[12]).

*This project has received funding from the European Union's Horizon 2020 research and innovation programme under grant agreement No **801305.***

3. Protocols to make colloidal NPs

3.1. Synthesis of colloidal $NaYF_4$ nanoparticles

3.1.1. Synthesis of colloidal $NaYF_4$ nanoparticles

Based on exemplary sample of Sm or Dy doped $NaYF_4$ colloidal nanoparticles, the synthesis protocol and basic characterization of the obtained materials is presented.

Preparation of Precursor: Stoichiometric amounts of lanthanide oxides (Y_2O_3, Nd_2O_3, Sm_2O_3 or Dy_2O_3 - 1×10^{-3}M) were mixed with 50% aqueous acetic acid. The mixture was transferred to a Teflon vessel and heated to 200 °C for 120 min under pressure, with the use of a stainless-steel hydrothermal autoclave. The final precursor was obtained by evaporation of residual acid and water in rotary evaporator, and further drying at 165 °C for 12 h.

Preparation of nanoparticles: In a typical synthesis procedure, the given amounts (2×10^{-3} M Ln^{3+}) of $(CH3COO)_3Ln$ lanthanide precursors were added to the three-neck flask with 12 ml OA and 30ml ODE. The solution was stirred under nitrogen atmosphere and heated slowly to 140 °C, followed by degassing under vacuum for 30 min to remove oxygen and water. After evaporation of residual water, the nitrogen atmosphere was maintained during the synthesis. Then, the reaction temperature was decreased to 50 °C, and during this time, solutions of ammonium fluoride (0.2964g) and sodium hydroxide (0.2g) dissolved in 10ml of methanol were added. Then, the temperature was increased to 75 °C and the mixture was kept at this temperature for 30 min to evaporate methanol. Subsequently, the reaction temperature was increased quickly to 300 °C. The reaction mixture was kept at this temperature for 30 min under nitrogen atmosphere. After the UCNPs formation the mixture was allowed to cool to room temperature. The UCNPs were precipitated by addition of ethanol and isolated by centrifugation at 10000 rpm for 10 min. For purification, the resulting pellet was dispersed in a minimal amount of *n*-hexane and again precipitated with excess ethanol. The UCNPs were isolated by centrifugation at 14000 rpm for 10 min. Finally, the purified core UCNPs were dispersed in $5cm^3$ chloroform.

*This project has received funding from the European Union's Horizon 2020 research and innovation programme under grant agreement No **801305.***

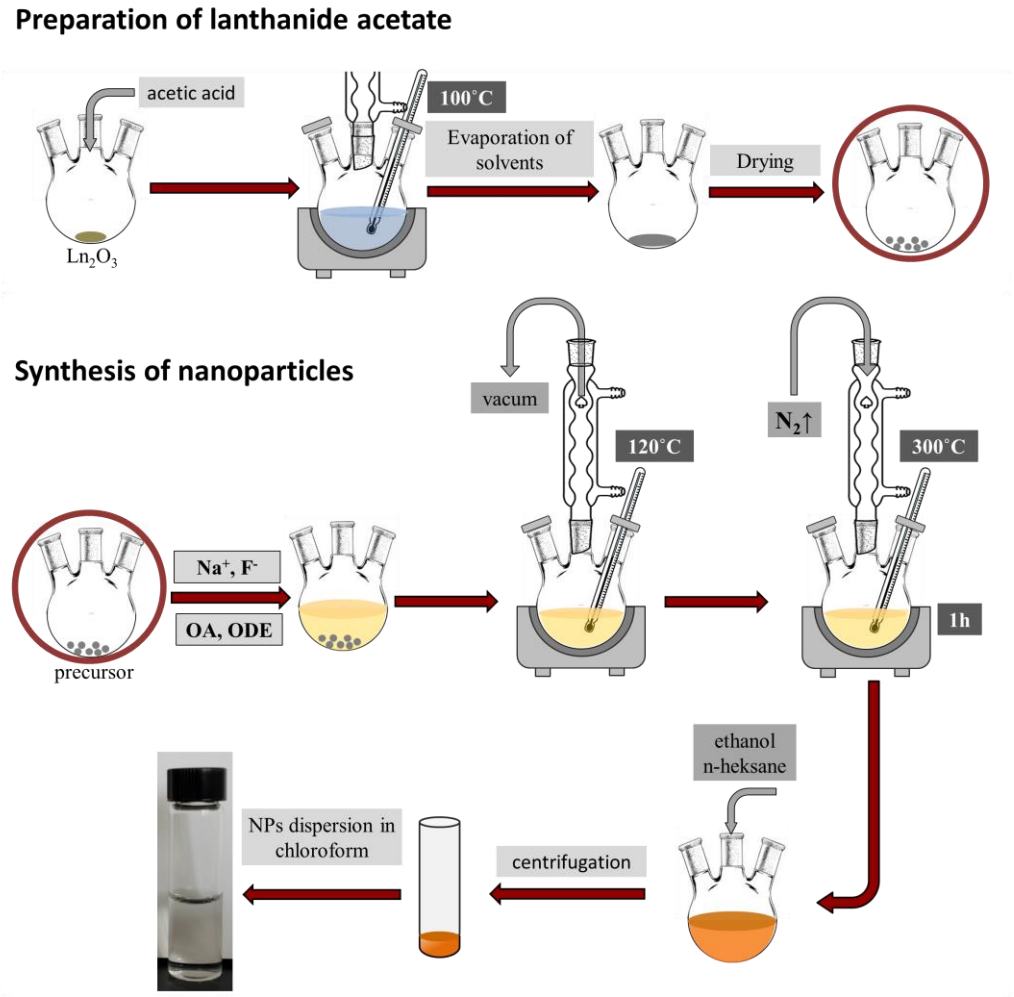

Fig.2. Schematic illustration of nanoparticle synthesis.

Table 1. Detailed precursor quantities used for Ln3+ doped NaYF4 colloidal nanoparticles synthesis.

Sample	Composition	Precursors		
		Nd_2O_3	Sm_2O_3	Dy_2O_3
FET_1	$NaNdF_4$	0.3364g	x	x
FET_2	$NaDyF_4$	x	x	0.3729g
FET_3	$NaSmF_4$	x	0.3487	x

*This project has received funding from the European Union's Horizon 2020 research and innovation programme under grant agreement No **801305.***

3.1.2. Analysis of structure (XRD), morphology (TEM) and colloidal properties (DLS)

According to Burns (J. H. Burns, Inorg. Chem., 1965, 4, 881–886) the hexagonal $NaYF_4$ structure belongs to the P6 group, where there is a nine-fold coordinated position occupied by Y^{3+}, another nine-fold occupied position occupied by Y^{3+}/Na^{+} (in the ratio 3 : 1) and a six-fold coordinated position occupied by Na^{+} and vacancies (ratio 1 : 1) (See Figure 3).

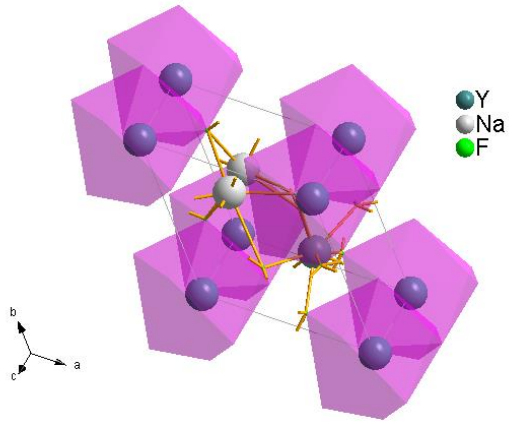

Figure 3. Visualization of hexagonal $NaYF_4$ structure

The phase purity and the high crystallization degree of synthesized nanocrystals were confirmed using XRD patterns (X-Ray Diffraction) analysis. A representative structural parameters of analyzed samples are enlisted in Table 2, representative TEM images and size distribution of the obtained nanoparticles are presented on Fig.4.

Table 2. Selected structural parameters obtained from XRD measurements

Sample	Grain size [nm]	a	c	strain	Rwp	Rp	Re	GOF
$NaNdF_4$	12.4	6.10441	3.71629	0.019	4.31	4.10	3.62	1.62
$NaDyF_4$	14.3	5.99209	3.56930	0.160	5.51	4.21	3.54	1.82
$NaSmF_4$	15.9	6.07195	3.65111	0.031	5.90	4.62	3.89	1.79

*This project has received funding from the European Union's Horizon 2020 research and innovation programme under grant agreement No **801305.***

3.1.3. DLS histograms showing size distribution

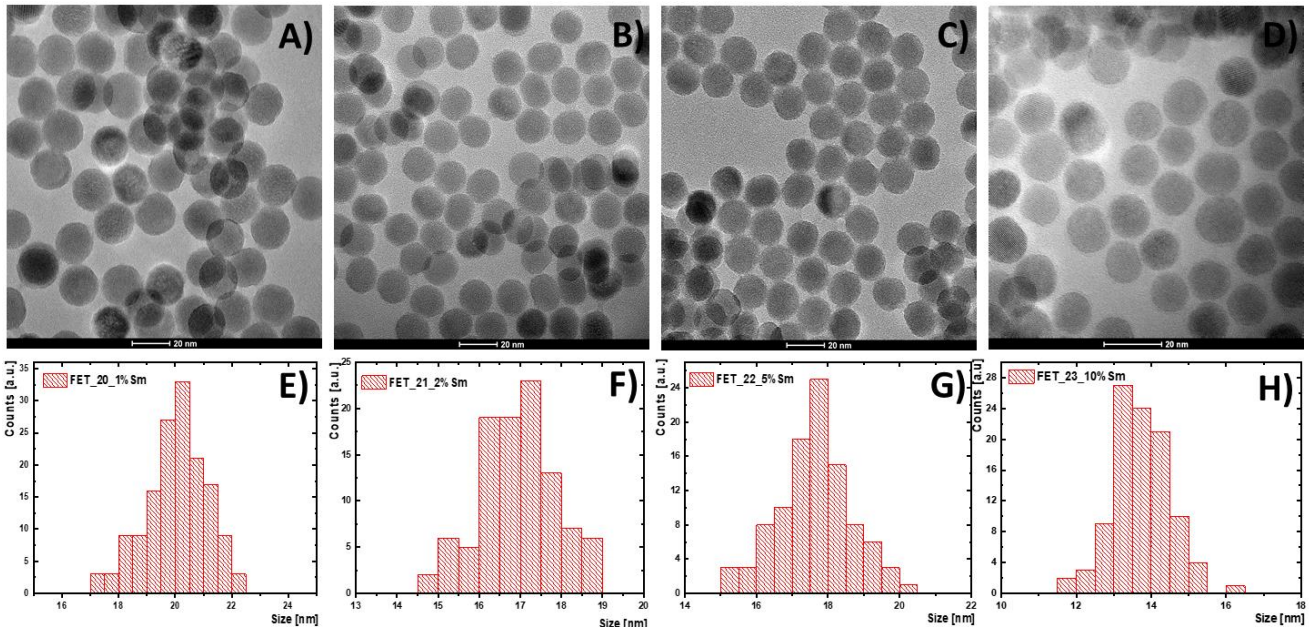

Figure 4. TEM images and size distribution histograms of NaYF:10%Yb^{3+} codoped with 1% (A and E), 2%(B and F), 5% (C and G) and 10% (D and H) of Sm^{3+}

3.1.4. Optical characterization of colloidal nanoparticles

So far, absorption spectra of the obtained samples have been measured (Fig.5-7). In the samples codoped with Nd^{3+} and Sm^{3+}, one may note optical transition typical for Nd^{3+} and Sm^{3+} ions. Especially interesting and perspective are the Nd^{3+} absorption bands, which lay in Near Infrared Spectral Region (NIR), i.e. $^4I_{9/2} \rightarrow {}^4F_{5/2}$ at 796 nm. The presence of Sm^{3+} built into the material was evidenced as well, but the role of Sm^{3+} is to non-radiatively convert the photons energy into heat. The energy level scheme of Nd^{3+}-Sm^{3+} and Nd^{3+}-Dy^{3+} should enable $Nd^{3+} \rightarrow Sm^{3+}$ / Dy^{3+} energy transfer (ET) highly probable, and due to numerous close by energy levels of Sm^{3+}/ Dy^{3+}, non-radiative depopulation should occur, under ~800 nm radiation. The Sm^{3+} doped samples (variable Sm^{3+} content) are studied at the moment and their spectral properties will be reported soon. For more precise description of the peaks on the absorption spectra, the absorption spectra of fully concentrated $NaNdF_4$, $NaSmF_4$, $NaDyF_4$ with ascribed all the peaks are shown below.

*This project has received funding from the European Union's Horizon 2020 research and innovation programme under grant agreement No **801305.***

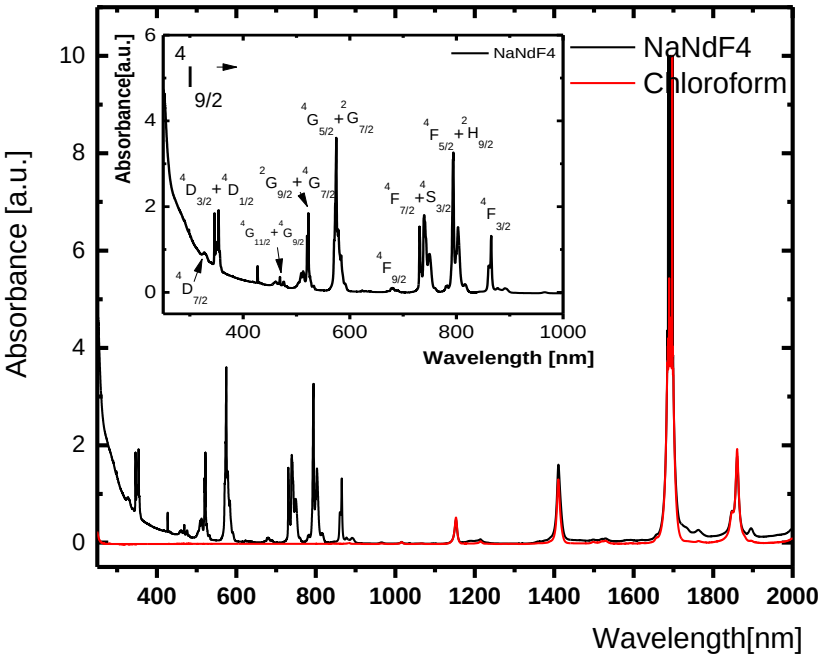

Figure 5. Absorption spectra of fully concentrated sodium neodymium fluoride ($NaNdF_4$).

*This project has received funding from the European Union's Horizon 2020 research and innovation programme under grant agreement No **801305.***

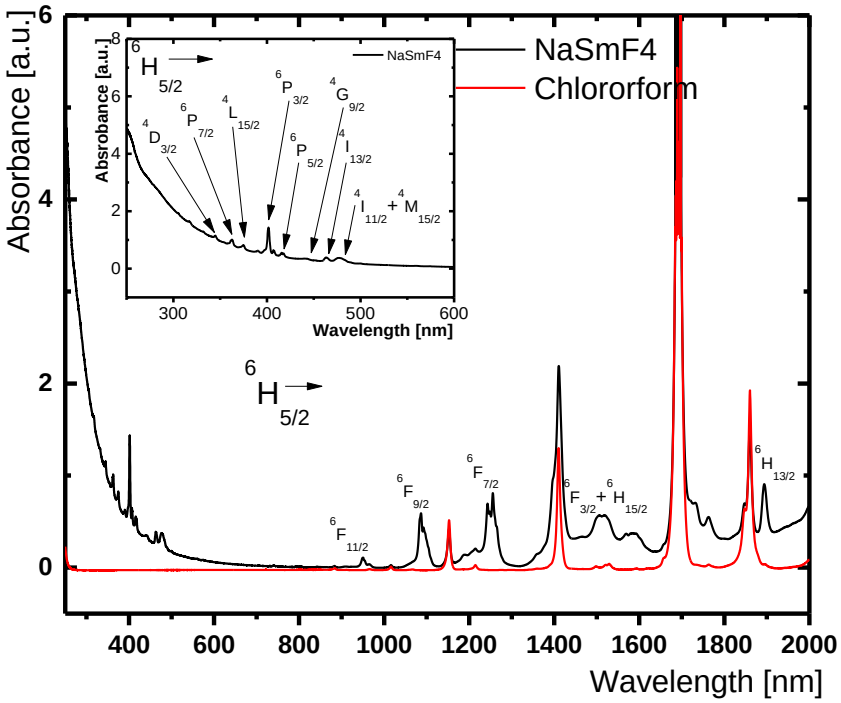

Figure 6. Absorption spectra of fully concentrated sodium samarium fluoride ($NaSmF_4$).

*This project has received funding from the European Union's Horizon 2020 research and innovation programme under grant agreement No **801305.***

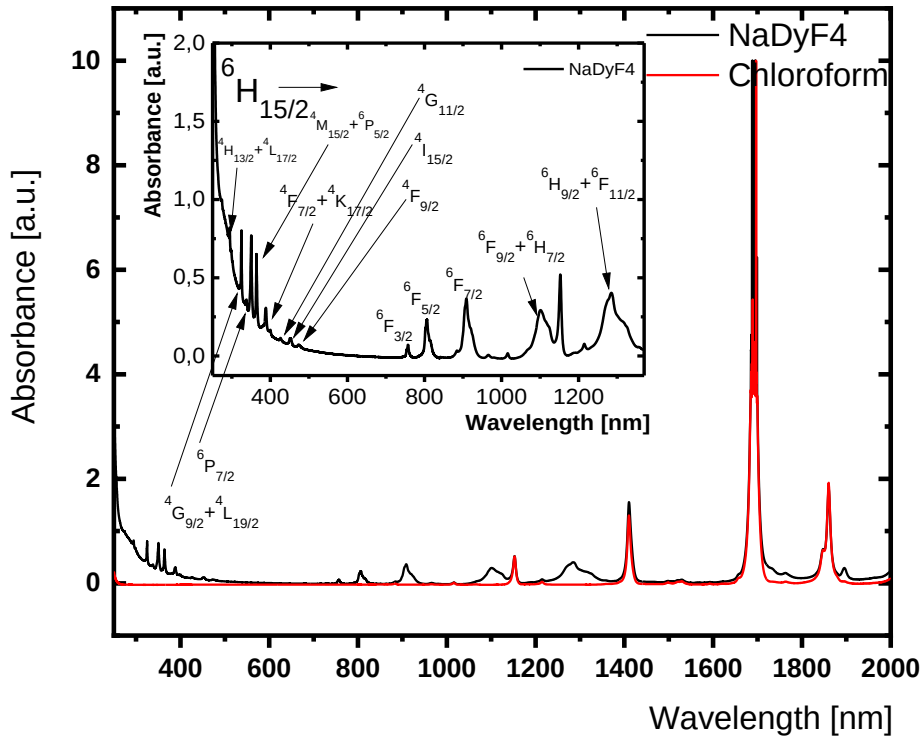

Figure 7. Absorption spectra of fully concentrated sodium dysprosium fluoride ($NaDyF_4$).

3.1.5. $NaYF_4$ NPs – changing ligands

During the synthesis of upconverting nanoparticles, the final product is dispersed in chloroform because of oleic ligand which are attached to the surface of UCNP's and make the hydrophobic. Chloroform is toxic for human body or cells so it is necessary to transfer the UCNP's to the water. There are couple methods to change the ligands, but we are using mainly two: (a) removing oleic acid ligands and (b)changing ligands to mercaptopropionic acid).

3.1.5.1. Removing oleic acid ligands with hydrochloric acid.

Procedure: 1ml of UCNPs in chloroform (ca 60 mg) was mixed with 5 ml HCl (pH= 4), then stirred vigorously 1 h for protonation of carboxyl groups. An aqueous phase was collected and washed twice by centrifugation and dispersed in water.

*This project has received funding from the European Union's Horizon 2020 research and innovation programme under grant agreement No **801305.***

Conclusions: the sample is slightly cloudy, stable in low pH, and should be stored in dark, decrease in emission intensity is observed.

3.1.5.2. Ligands exchange to 3-mercaptopropionic acid

Procedure: 0.5ml of UCNPs in chloroform was mixed with 1 ml of chloroform and 2 ml of 3-mercaptopropionic acid. The mixture was stirred vigorously for 12 hours at room temperature. After stirring overnight, 2 mL of distilled and stirred again for 3 hours in room temperature.
The turbid solution obtained was centrifuged, and the pellet was redispersed in 3ml of distilled water.
Conclusions: the sample is slightly cloudy, stable, decrease in emission intensity is observed.

3.1.6. Conclusions

- $NaNdF_4$ shows most intense and multiple absorption bands (absorbance ~1-3.5) in the visible and NIR spectral region, which is important to effectively absorb the photoexcitation
- Sm^{3+} shows reasonable absorption at around 1100, 1250, 1500-1600nm (absorbance >0.5)
- Dy^{3+} shows absorption at 800, 900, 1100,1300 nm but the absorbance is low <0.5)
- It may be reasonable to combine 2 or 3 ions to get efficient heating, e.g. Nd^{3+} as absorber at 800 nm and Sm^{3+} with Dy^{3+} as non-radiative heat generators
- The original colloidal $NaYF_4$ NPs with original Oleic Acid capping ligands assure good colloidal stability (over a year), good transparency an d narrow size distribution of NPs
- Changing the ligands to MPA make them very stable and enable to get water colloids, but the protocol is much longer than removing ligands with hydrochloric acid
- Removing ligands enable to get water colloids, but the NPs should be stored in dark, and require acidic environment (low pH), the protocol is simply and easy
- Colloidal stability $NaNdF_4$ sample tends to aggregate, pink color is caused by Nd^{3+} ions. Other samples ($NaSmF_4$ and $NaDyF_4$) do not aggregate and no sediment is visible. There is no visible difference in a 3 month period of time before and after synthesis.

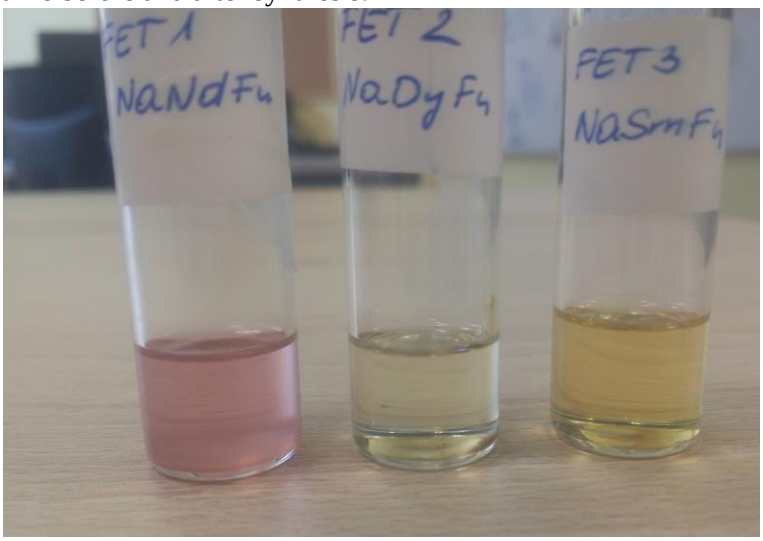

Figure 8. Samples FET_1-3 after 3 months period of time

*This project has received funding from the European Union's Horizon 2020 research and innovation programme under grant agreement No **801305.***

3.1.7. Further investigation

1. The protocols and ligands exchange as well as raw Ln^{3+} co-doped $NaYF_4$ nanoparticles have been transferred to partner CNRS (on May 13th 2019) for further bio-functionalization protocol development.
2. Further optical spectroscopy studies will be performed to understand the role of dopant concentration on luminescent and light-to-heat conversion efficiency properties of the obtained materials.

3.2. Synthesis of colloidal AuNPs

Au nanoparticles were prepared by reduction in the gold salt with sodium citrate[13,14]. Freshly prepared water solution of sodium citrate was added to 9.95 ml of water solution of $HAuCl_4$ in constant temperature (80°C) under vigorous stirring. The color of the mixture turned wine red after few minutes which indicate the production of Au nanoparticles.

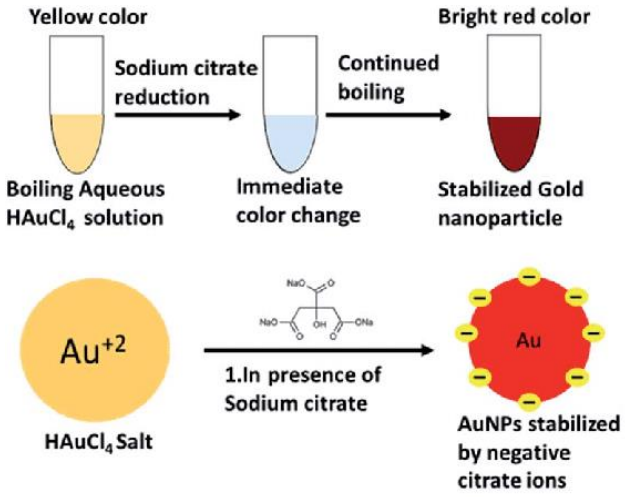

Figure 9. Scheme of synthesis Au Np's[15]

A series of materials were prepared as presented in Table 3, i.e. In function of sodium citrate solution amount. To observe any differences in size the absorption spectra were collected.

*This project has received funding from the European Union's Horizon 2020 research and innovation programme under grant agreement No **801305.***

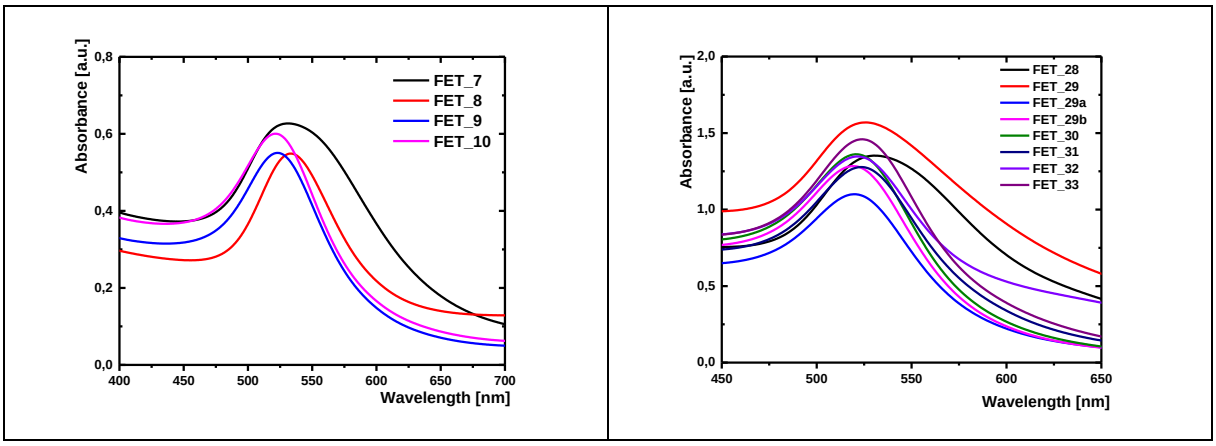

Figure 10. The absorption spectra of different AuNPs (Table 3).

Based on literature [14] as well as other links [a,b] the average size of obtained materials based on maximum intensity of surface plasmon resonance of Au nanoparticles was estimated.

Table 3. The composition or precursors and average size of Au NP's:

Sample	Composition	Sodium citrate solution		Maximum at [nm]	Estimated size [nm]
		Concentration	Amount		
FET_7	AuNP's	0.34M	47µl	543	50
FET_8	AuNP's	0.34M	23µl	534	50
FET_9	AuNP's	0.34M	94µl	523	20
FET_10	AuNP's	0. 34M	188µl	520	15
FET_28	AuNP's	0.085M	47µl	534	50
FET_29	AuNP's	0.17M	47µl	528	40
FET_30	AuNP's	0.34M	47µl	520	15
FET_31	AuNP's	0.425M	47µl	523	15/20
FET_32	AuNP's	0.51M	47µl	521	15
FET_33	AuNP's	0.68M	47µl	524	20

*Samples FET_28-FET_33 was made with different solution of $HAuCl_4$ with concentration around 0.36M.

[a] https://www.sigmaaldrich.com/technical-documents/articles/materials-science/nanomaterials/gold-nanoparticles.html

[b] http://www.cytodiagnostics.com/store/pc/Gold-Nanoparticle-Properties-d2.htm

*This project has received funding from the European Union's Horizon 2020 research and innovation programme under grant agreement No **801305.***

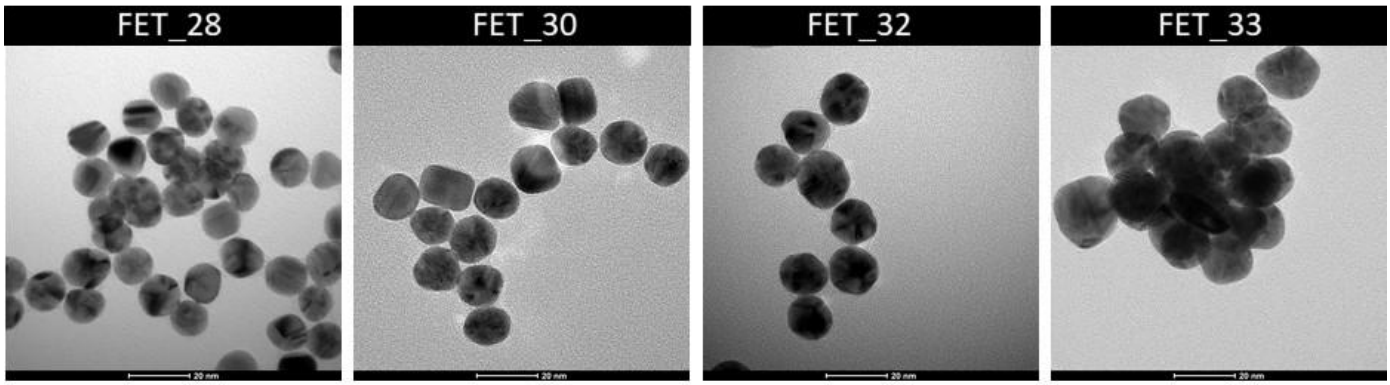

Figure 11. TEM images of synthesized Au nanoparticles

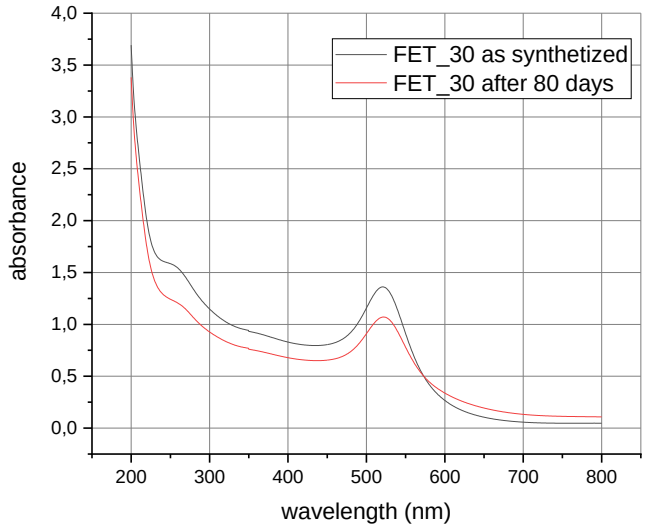

Figure 12. Change of absorption spectra of AuNPs after 80 days - data for FET_30 sample

*This project has received funding from the European Union's Horizon 2020 research and innovation programme under grant agreement No **801305.***

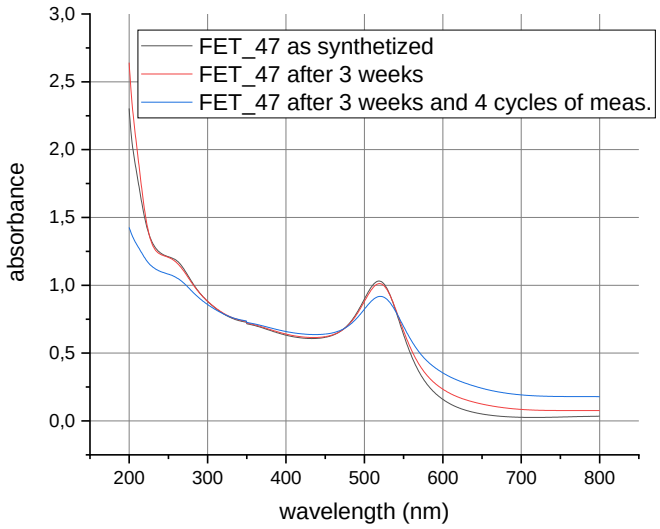

Figure 13. Change of absorption spectra of AuNPs after 3 weeks and laser irradiation - data for FET_47 sample

3.2.1. Conclusions

- With increasing the amount of sodium citrate solution decreasing of the size of the AuNP's nanoparticles is observed.
- Colloidal Au nanoparticles have a low stability in time. After 3 month period of time there is a visible difference in sample color intensity, also there is a violet sediment in the bottom of a sample. As-prepared colloidal Au nanoparticles are stable, but they are degrading in time. After 3 months period of time there is a visible difference in sample color intensity, also there is a violet sediment in the bottom of a sample. Absorption spectra shows that after 3 weeks there is only slight decrease of absorption in the visible range, but after 80 days the decrease is significant. Also the influence of 532 nm irradiation was tested (4 cycles of 35 min irradiation with power density 200 mW/cm^2) and it shows that absorption peak near 514nm slightly but noticeably decrease.
- Comparing the values obtained from literature with experimental values obtained from TEM measurements the great consistency is observed. The one exception is sample FET_28.

3.3. Synthesis of colloidal polystyrene nanoparticles

Several methods for synthesis polystyrene (PS) nanoparticles have been developed, such as emulsion polymerization, emulsifier free polymerization, precipitation polymerization and dispersion polymerization.[16] In the literature can be found a synthesis methods for obtain polystyrene in nanosized as well as much bigger polystyrene microbeads. The polystyrene nanoparticles could be also modified. For example, A.M. Nuruzatulifah synthesized nanosized polystyrene spheres with

*This project has received funding from the European Union's Horizon 2020 research and innovation programme under grant agreement No **801305.***

fluorescent dye attached to the surface.[16] Yunxing Li et al. covered the as prepared nanoparticles of polystyrene with nobel metals as Au, Ag, Pt or Pd.[17] Anna E. Guller in her work showed that the polystyrene beads can also be covered by upconverting nanoparticles.[18] And H. Qian with his group even incorporated the UCNP's inside the polystyrene nanospheres.[19]

If there is so much different ways to modificate the polystyrene nanoparticles such as attaching molecules to the surface or incorporating them inside the nanoparticles it could be interesting to synthesized a polystyrene 'hybrid' with two different nanomaterials inside.

At first we tried to obtain bare nanopolystyrene beads. Based on work of H. Qian[19] we obtained a homogenous polystyrene nanospheres with very narrow distribution and size around 100nm. We also made first steps with incorporating the different nananoparticles to the PS nanospheres, such as UCNP's, Si nanoparticles and Au nanoparticles.

3.3.1. Synthesis protocol

1ml of liquid styrene was mixed with 1ml of cyclohexane. The as prepared mixture was added to water solution (50ml) of 0.08g sodium dodecyl sulfate (SDS). After that the obtained solution was treated using ultrasound for 15 minutes to obtain a miniemulsion. Subsequently the solution was transferred to 250ml three neck reaction flask and stirred. The 0.02g of pottasium peroxydisulfate wass added to reaction flas and the obtained mixture was stirred under nitrogen atmosphere for 10 minutes. After that the temperature of reaction was increased to 80^{o}C. The soolution was maintained at this temperature for 24 hours. After that the polystyrene nanospheres were collected by centrifugation (14 000rpm, 10min) and dispersed in 10 ml of water.

*This project has received funding from the European Union's Horizon 2020 research and innovation programme under grant agreement No **801305.***

3.3.2. Analysis of morphology (SEM) and colloidal properties (DLS)

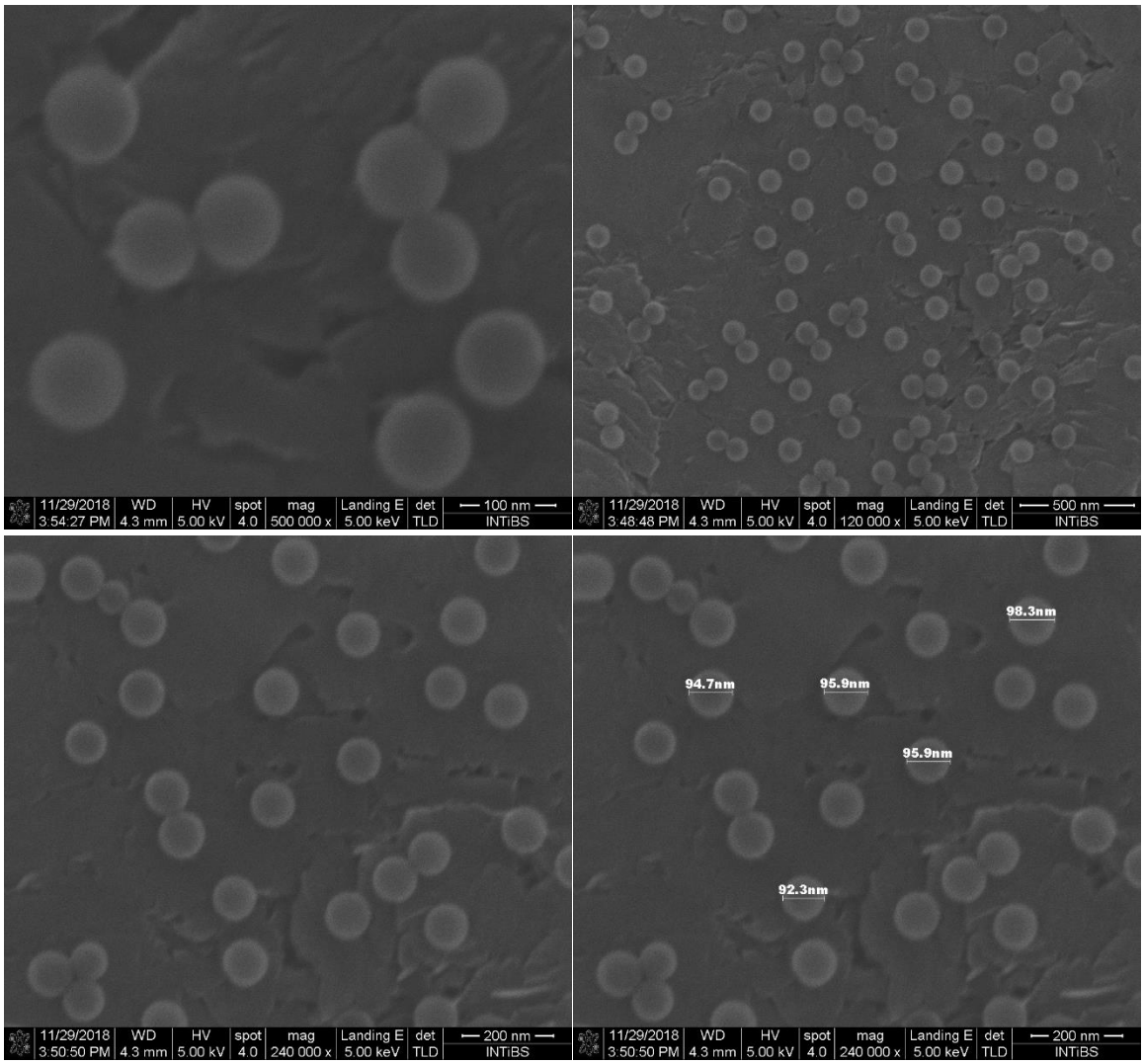

Figure 14. SEM image of nanosized polystyrene beads.

To check the influence of the initiator of polymerization the amount of potassium peroxydisulfate was increased to 0.04g

*This project has received funding from the European Union's Horizon 2020 research and innovation programme under grant agreement No **801305.***

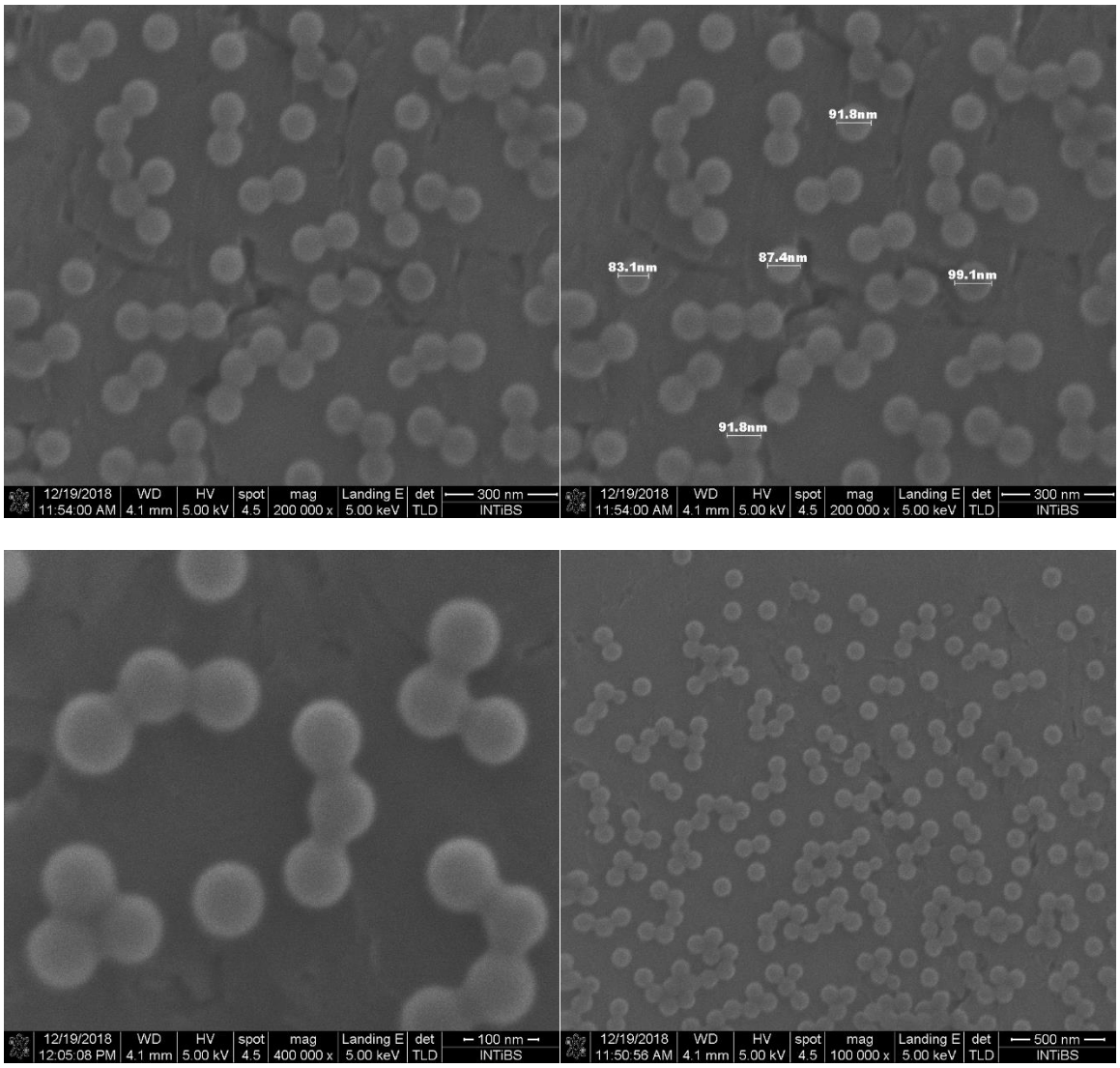

Figure 15. SEM image of nanosized polystyrene beads with increased amount of potassium peroxydisulfate.

Next we have tried to incorporate the UCNP's, SiNP's and AuNp's to the polystyrene nanospheres by adding the solutions of each nanoparticles to the reaction mixture. We added 1ml of UCNP;s, and 0,5 ml of AuNP's and SiNP's to the solution containing cyclohexane and liquid styrene. The rest steps of the synthesis was the same as before.

*This project has received funding from the European Union's Horizon 2020 research and innovation programme under grant agreement No **801305.***

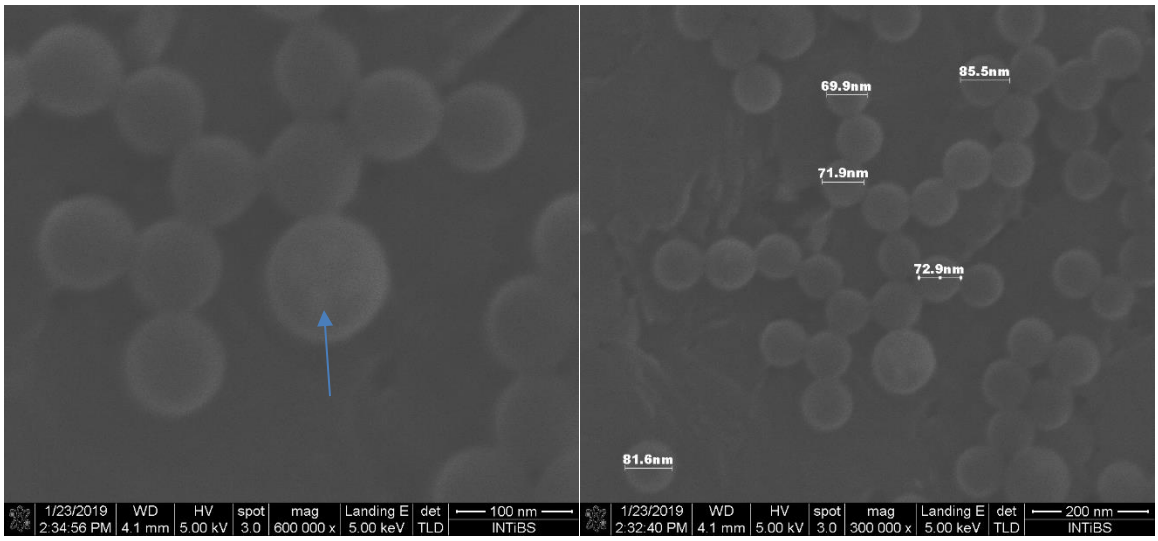

Figure 16. SEM image of nanosized polystyrene beads with UCNPS inside (indicated by arrow)

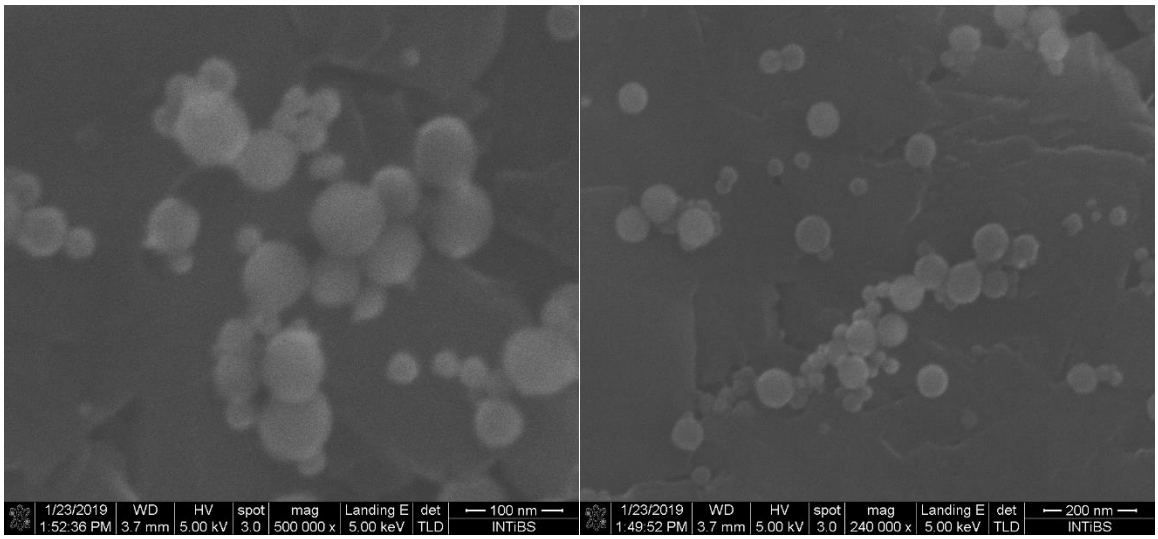

Figure 17. SEM image of nanosized polystyrene beads with AiNPs inside – it seems the SiNPs do not get into PS host.

*This project has received funding from the European Union's Horizon 2020 research and innovation programme under grant agreement No **801305.***

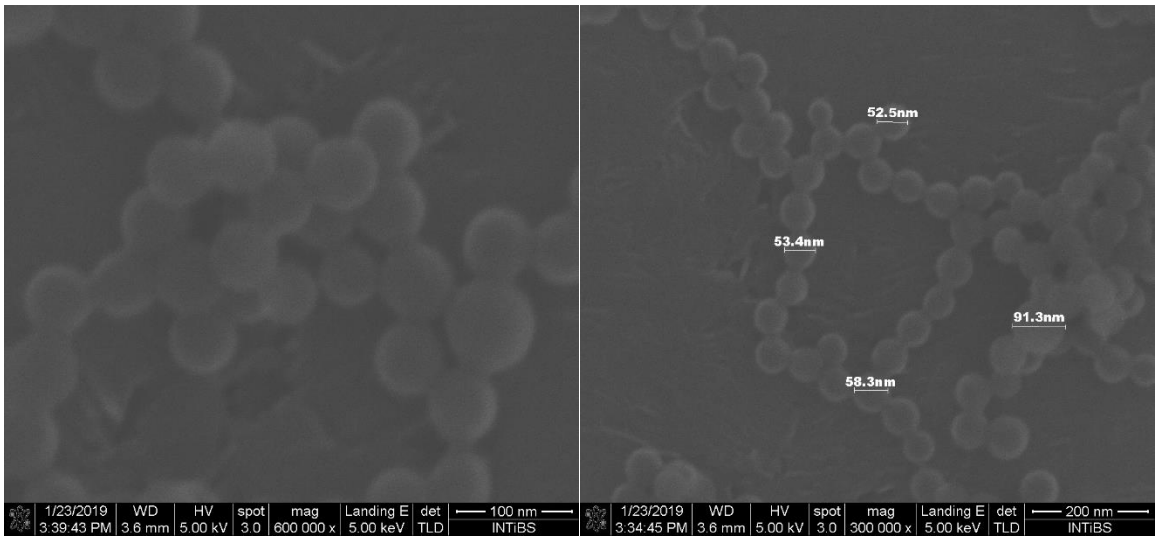

Figure 18. SEM image of nanosized polystyrene beads with AuNPs inside.

3.3.3. Conclusions

- Regular and narrow size distributed polystyrene nanobeads were successfully synthesized
- It seems UCNPs ($NaYF_4$ NPs) were successfully build into the PS beads, which however requires further optimization
- It seems SiNPs are not covered with PS – the images show separate SiNPs and PS beads
- It is not possible to equivocally determine if AuNPs are built into PS beads. TEM images will be shortly performed to confirm that in electron transmission mode.
- The nanobeads are very stable water colloids, after weeks, even months there is no sedimentation observed
- Only in the sample with Si Np's the sedimentation is observed. The reason for that SiAu Np's are much bigger than AuNP's and not very stable

3.3.4. Future work:

- Further optimization of PS and NP+PS compositions to keep single NPs within single PS bead.

3.4. Fe^{3+}-doped $Y_3Al_5O_{12}$ (YAG) and $Y_3Fe_5O_{12}$ (YIG) powders

Introduction: In the previous deliverable (D1.1_Del1_First Generation of Nanoparticles) modified Pechini synthesis of Fe^{3+}-doped $Y_3Al_5O_{12}$ (YAG) and $Y_3Fe_5O_{12}$ (YIG) powders with detail synthesis procedure, X-ray diffraction, diffuse reflectance, transmission electron microscopy as well as hyperthermia measurements under magnetic field is reported. Further plan was to disperse obtained powders into stabile suspension for additional magnetic hyperthermia measurements and comparison with iron-oxide nanoflowers and nanospheres suspension.

*This project has received funding from the European Union's Horizon 2020 research and innovation programme under grant agreement No **801305.***

Powder-to-colloid procedure: In order to prepare stabile colloid suspension further procedure is established and given in detail (see Scheme 1):

Mix 0.1 g powder with 19.2 ml H_2O and 0.8 ml of 2.6 M aqueous solution of citric acid. Under slow stirring adjust pH value to 5.1 by adding conc. NH_4OH dropwise. Reflux obtained mixture at 80°C for 90 minutes under magnetic steering. After cooling to the room temperature again adjust pH to 10.1 by adding conc. NH_4OH dropwise under slow stirring. Centrifugate the mixture at 3000 rpm for 2 minutes. Remove supernatant. Mix obtained sediment with 12.5 ml H_2O and expose it for 1 minute to the ultasonic horn at 40% power. Centrifugate obtained mixture at 5000 rpm for 3 minutes. Now, suprnatant, i.e. nanoparticles dispersed in aqueous media, are ready for futher characterization and measurements, while sediment should be removed.

Exact concentration (mg/ml) of nanoparticles in the obtained colloid needs to be determined (by thermogravimetry for example).

Further investigation:

- powder samples given in the "D1.1_Del1_First Generation of Nanoparticles" will be dispersed according to the given powder-to-colloid procedure and compared with iron-oxide nanoflowers and nanospheres suspension
- additional $Gd_3Fe_5O_{12}$ and $Y_3Al_{2.5}Fe_{2.5}O_{12}$ samples are synthesized and will be dispersed according to the given powder-to-colloid procedure and compared with all the samples.

*This project has received funding from the European Union's Horizon 2020 research and innovation programme under grant agreement No **801305.***

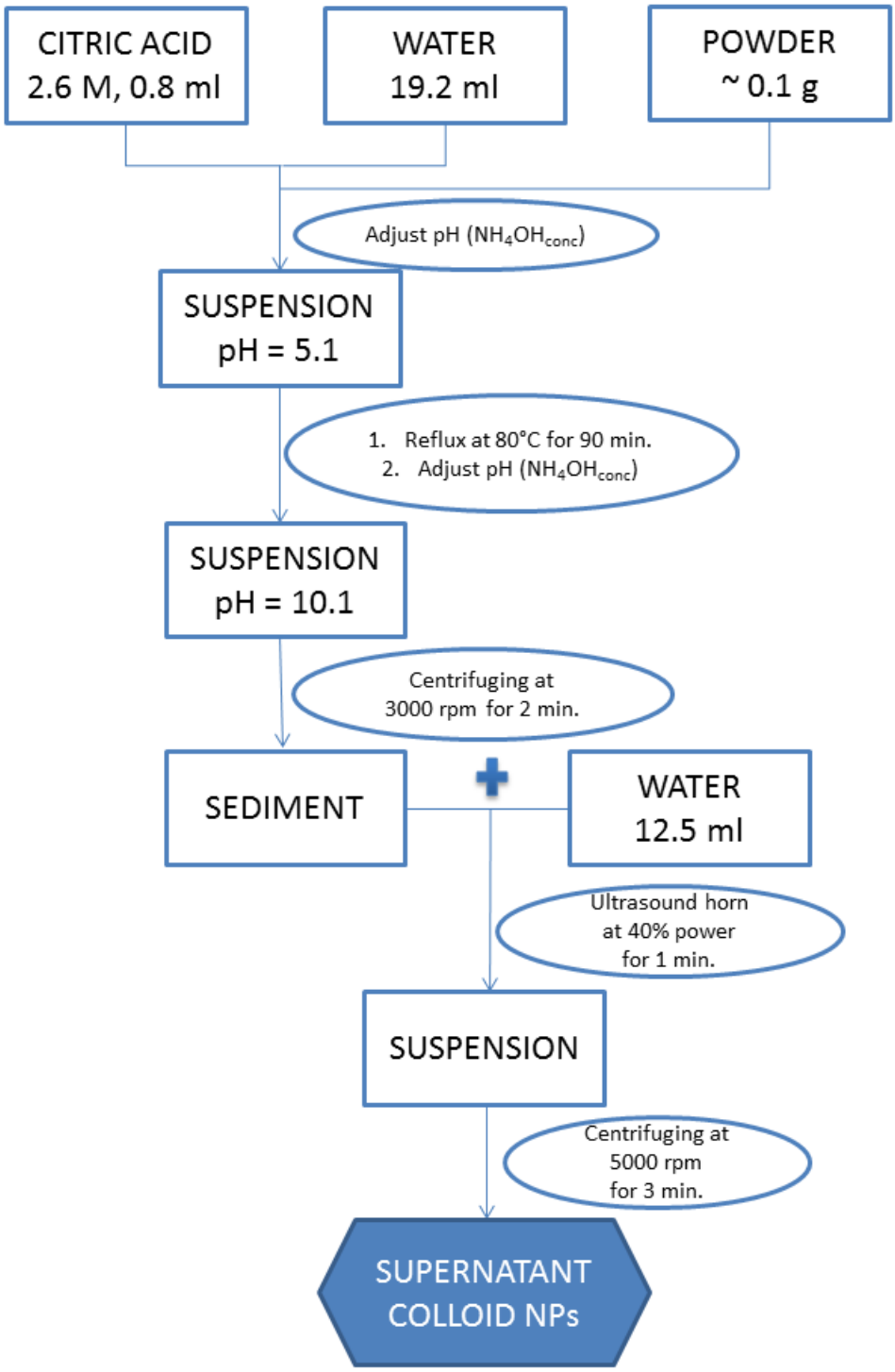

Scheme 1 Powder-to-colloid procedure

*This project has received funding from the European Union's Horizon 2020 research and innovation programme under grant agreement No **801305.***

4. Biofunctionalization

In order to study the comportment of NH/NT in solution, and compare the different systems between them, a common way of functionalization has to be determined.

The active targeting described in the proposal goes through the use of monoclonal antibody targeting the epithelial growth factor receptor (EGFR), overexpressed in cancer cell lines. Cetuximab and Nemotuzumab have been chosen for this purpose, although they have first been described for therapeutic purpose[20]. Their advantages for active targeting rely on their higher affinity to EGFR compared to endogenous ligands. Furthermore, a therapeutic synergic effect has been determined when linked to NPs[21].

In order to link the antibodies to the NPs, a binding site has to be generated. For this purpose, carbohydrate located on the glycoxidation sites of the heavy chain can be oxidized to create reactive aldehydes. Those soft and controlled oxidation are widely available in the literature[22,23].

On the other hand, active sites also have to be generated on the NPs counterpart. Usually terminally amine group are introduced at the end of a hydrophilic polymer chain. This allows the creation of peptidyl link between the NP and the antibody, while the polymer chain will prevent the adsorption of plasma's proteins (poly ethylene glycol, PEG, for example). The main challenge consists in adding those polymer chains on the surface of the NPs.

To do so, NPs can be divided into two main categories: the oxygen containing NPs and the non-oxygen containing NPs.

The oxygen containing NPs (YIG, YAG, ZGO, SPIONs) present hydroxyl groups on the surface, which constitutes a suitable starting group for functionalization. The density of those groups on the surface can be increased with several steps, including milling and slow acidic/basic attack. Once the wanted density obtained, a silane anchor group with a more powerful nucleophile group can be added. Finally, an activated polymer, such as NHS-PEG-NH2/COOH, can easily coat the nanoparticles. Such works have been described by the French partners[24], but are also reported for YAG NPs[25].

Concerning the non-containing oxygen NPs, the functionalization has to be determined depending on the surface state. To this date, bibliographical research has been done on Ag2S NPs.

Ag2S NPs can follow two distinct functionalization pathways. The first one is using a common synthesis approach in organic solvent. Indeed, their synthesis are most often taking place in organic solvent with the use of aliphatic chains to stabilize the obtained NPs. Literature have then described several ligand exchange processes with thiolated polymer, such as SH-PEG. Such technics have also been described for Ag2Se NPs[23]. The second one consists in directly using a thiolated polymer as sulfur source for the NPs synthesis[26–28].

The functionalization method will be chosen depending on the synthesis developed by the LCMCP partners and on the resulting properties of the different Ag2S NPs.

*This project has received funding from the European Union's Horizon 2020 research and innovation programme under grant agreement No **801305.***

These functionalization pathways are suitable for an injection of a NH-NT mix. After injection, we can assume than both NPs, with the same size and coating, will behave the same and efficiently targeting tumors. Nevertheless, a common formulation can also be investigated following different possibilities:

- Use of a silica shell encapsulating NH-NT mix[29]
- Use of a lysosome encapsulation[30]
- Use of PEG-biotin functionalization forming a network with the use of streptavidin[31]

These options can also be taking into account, although the size of this kind of assembly could be a major issue for tumor targeting.

5. General conclusions and future work

The development of the materials is in progress, and number of different approaches to make colloidal nanoparticles have been taken. In most cases, the synthesis protocols were selected, which by definition make colloidal nanoparticles (e.g. chloroform or water, $NaYF_4$ or AuNPs, respectively), which require developing of protocols to bring the colloidal NPs to buffer solution for further biofunctionalization.

Further work include:

- Verification of colloidal stability of AuNPs after evaluation procedure of light-to-heat conversion (we found out the intense laser beam may change the properties of the colloidal AuNPs) (WPAS)
- Further optimization of PS and NP+PS compositions to keep single NPs within single PS bead (WPAS)
- Individual biofunctionalization procedures are under development for specific classes of materials (AuNPs, Ag_2S, $NaYF_4$, PS etc.) (CNRS), that will be used in all further work. This will help e.g. WPAS and VINCIA partners, to develop new compositions, and in parallel the bio-functionalization protocols (CNRS) will be developed and ready to bring the most promising NPs from chemical labs to in-vitro and in-vivo experiments.

*This project has received funding from the European Union's Horizon 2020 research and innovation programme under grant agreement No **801305.***

6. References

1. Lohse, S. E. & Murphy, C. J. Applications of Colloidal Inorganic Nanoparticles: From Medicine to Energy. *J. Am. Chem. Soc.* **134,** 15607–15620 (2012).

2. Zhang, Y.-W., Sun, X., Si, R., You, L.-P. & Yan, C.-H. Single-Crystalline and Monodisperse LaF3 Triangular Nanoplates from a Single-Source Precursor. *J. Am. Chem. Soc.* **127,** 3260–3261 (2005).

3. Mai, H.-X. *et al.* High-Quality Sodium Rare-Earth Fluoride Nanocrystals: Controlled Synthesis and Optical Properties. *J. Am. Chem. Soc.* **128,** 6426–6436 (2006).

4. Bogdan, N., Vetrone, F., Ozin, G. A. & Capobianco, J. A. Synthesis of Ligand-Free Colloidally Stable Water Dispersible Brightly Luminescent Lanthanide-Doped Upconverting Nanoparticles. *Nano Lett.* **11,** 835–840 (2011).

5. Wang, F. *et al.* Tuning upconversion through energy migration in core–shell nanoparticles. *Nat. Mater.* **10,** 968–973 (2011).

6. Chen, Z. *et al.* Versatile Synthesis Strategy for Carboxylic Acid−functionalized Upconverting Nanophosphors as Biological Labels. *J. Am. Chem. Soc.* **130,** 3023–3029 (2008).

7. Zhang, H. *et al.* Plasmonic Modulation of the Upconversion Fluorescence in NaYF4:Yb/Tm Hexaplate Nanocrystals Using Gold Nanoparticles or Nanoshells. *Angew. Chemie Int. Ed.* **49,** 2865–2868 (2010).

8. Palo, E. *et al.* Effective Shielding of NaYF4:Yb3+,Er3+ Upconverting Nanoparticles in Aqueous Environments Using Layer-by-Layer Assembly. *Langmuir* **34,** 7759–7766 (2018).

9. Chen, Z. *et al.* Construction of nanoparticle superstructures on the basis of host–guest interaction to achieve performance integration and modulation. *Phys. Chem. Chem. Phys.* **14,** 6119–6125 (2012).

10. Sedlmeier, A. & Gorris, H. H. Surface modification and characterization of photon-upconverting nanoparticles for bioanalytical applications. *Chem. Soc. Rev.* **44,** 1526–1560 (2015).

11. Duong, H. T. T. *et al.* Systematic investigation of functional ligands for colloidal stable upconversion nanoparticles. *RSC Adv.* **8,** 4842–4849 (2018).

12. Gnach, A. & Bednarkiewicz, A. Lanthanide-doped up-converting nanoparticles :

13. Kobayashi, Y. *et al.* Control of shell thickness in silica-coating of Au nanoparticles and their X-ray imaging properties. *J. Colloid Interface Sci.* **358,** 329–333 (2011).

14. Wolfgang Haiss, *,†,‡, Nguyen T. K. Thanh, †,‡, Jenny Aveyard, † and & Fernig‡, D. G. Determination of Size and Concentration of Gold Nanoparticles from UV−Vis Spectra.

*This project has received funding from the European Union's Horizon 2020 research and innovation programme under grant agreement No **801305.***

(2007). doi:10.1021/AC0702084

15. Saraf, N. *et al.* Colorimetric detection of epinephrine using an optimized paper-based aptasensor. *RSC Adv.* **7,** 49133–49143 (2017).

16. Nuruzatulifah, A. M., Nizam, A. A. & Ain, N. M. N. Synthesis and Characterization of Polystyrene Nanoparticles with Covalently Attached Fluorescent Dye. *Mater. Today Proc.* **3,** S112–S119 (2016).

17. Bhattarai, S., Kim, J. S., Yun, Y. S. & Lee, Y. S. Preparation of polyaniline-coated polystyrene nanoparticles for the sorption of silver ions. *React. Funct. Polym.* **105,** 52–59 (2016).

18. Guller, A. E. *et al.* Cytotoxicity and non-specific cellular uptake of bare and surface-modified upconversion nanoparticles in human skin cells. *Nano Res.* **8,** 1546–1562 (2015).

19. Qian, H., Li, Z. & Zhang, Y. Multicolor polystyrene nanospheres tagged with up-conversion fluorescent nanocrystals. *Nanotechnology* **19,** (2008).

20. Berger, C., Krengel, U., Stang, E., Moreno, E. & Helene Madshus, I. Nimotuzumab and Cetuximab Block Ligand-independent EGF Receptor Signaling Efficiently at Different Concentrations. *J. Immunother.* **34,** 550–555 (2011).

21. García-Fernández, L. *et al.* Conserved effects and altered trafficking of Cetuximab antibodies conjugated to gold nanoparticles with precise control of their number and orientation. *Nanoscale* **9,** 6111–6121 (2017).

22. Chu, I.-M., Tseng, S.-H. & Chou, M.-Y. Cetuximab-conjugated iron oxide nanoparticles for cancer imaging and therapy. *Int. J. Nanomedicine* **10,** 3663 (2015).

23. Zhu, C.-N. *et al.* Near-Infrared Fluorescent Ag_2Se-Cetuximab Nanoprobes for Targeted Imaging and Therapy of Cancer. *Small* **13,** 1602309 (2017).

24. Maldiney, T., Rémond, M., Bessodes, M., Scherman, D. & Richard, C. Controlling aminosilane layer thickness to extend the plasma half-life of stealth persistent luminescence nanoparticles in vivo. *J. Mater. Chem. B* **3,** 4009–4016 (2015).

25. Sengar, P., Hirata, G. A., Farias, M. H. & Castillón, F. Morphological optimization and (3-aminopropyl) trimethoxy silane surface modification of Y3Al5O12:Pr nanoscintillator for biomedical applications. *Mater. Res. Bull.* **77,** 236–242 (2016).

26. Asik, D., Yagci, M. B., Demir Duman, F. & Yagci Acar, H. One step emission tunable synthesis of PEG coated Ag_2S NIR quantum dots and the development of receptor targeted drug delivery vehicles thereof. *J. Mater. Chem. B* **4,** 1941–1950 (2016).

27. Santos, H. D. A. *et al.* Time resolved spectroscopy of infrared emitting Ag_2S nanocrystals for subcutaneous thermometry. *Nanoscale* **9,** 2505–2513 (2017).

28. Zhang, Y. *et al.* Affibody-functionalized Ag_2S quantum dots for photoacoustic imaging of

*This project has received funding from the European Union's Horizon 2020 research and innovation programme under grant agreement No **801305.***

epidermal growth factor receptor overexpressed tumors. *Nanoscale* **10,** 16581–16590 (2018).

29. Teston, E. *et al.* Nanohybrids with Magnetic and Persistent Luminescence Properties for Cell Labeling, Tracking, In Vivo Real-Time Imaging, and Magnetic Vectorization. *Small* **14,** 1800020 (2018).

30. Liu, J. Interfacing Zwitterionic Liposomes with Inorganic Nanomaterials: Surface Forces, Membrane Integrity, and Applications. *Langmuir* **32,** 4393–4404 (2016).

31. Scott, A. W., Garimella, V., Calabrese, C. M. & Mirkin, C. A. Universal Biotin–PEG-Linked Gold Nanoparticle Probes for the Simultaneous Detection of Nucleic Acids and Proteins. *Bioconjug. Chem.* **28,** 203–211 (2017).

*This project has received funding from the European Union's Horizon 2020 research and innovation programme under grant agreement No **801305.***